Accounting for the heat island effect in building energy simulation: a case study in Wuhan, China

Long Pei, Patrick Schalbart, Bruno Peuportier

Accounting for the heat island effect in building energy simulation: a case study in Wuhan, China

Long PEI [1], Patrick SCHALBART[1], Bruno PEUPORTIER[1]
[1] MINES ParisTech, PSL Research University, CES - Centre d'efficacité énergétique des systèmes, 60 Bd St Michel 75006 Paris, France

Abstract

The climate data used for dynamic energy simulation of buildings located in urban areas are usually collected in meteorological stations situated in rural areas, which do not accurately represent the urban microclimate (e.g. urban heat island effect), leading to potential simulation errors. This paper aims at quantitatively evaluating the effects of heat island on a high-rise building energy performance, based on the microclimate simulation tool ENVI-met and building energy simulation tool COMFIE. However the computation of microclimate is time consuming; it is not possible to simulate every day of a year in a reasonable time. This paper proposes a method that generates hourly "site-specific climate data" to avoid long microclimate simulation time. A coupling method of ENVI-met and COMFIE was developed for more precise simulation, considering the effects of heat island on buildings energy performance. It was applied to a high-rise building in Wuhan, China. The results showed that the yearly average urban heat island effect intensity at the height of 3 m was estimated to be 0.45 °C and decreased with the height. Compared to the simulation considering the outdoor temperature variation with the height and orientation, using the original climate data collected in rural areas led to an overestimation of the heating load by around 3.5 % and an underestimation of the cooling load by around 3.9 %. Compared to the weather file at the height of 3 m in the south neglecting the temperature variation along the height, the heating load was overestimated by 5.4 % and the cooling load was underestimated by 6.9 %. The methods proposed in this paper can be used for a more precise application of urban building energy simulation.

Keywords: Heat island effect; high-rise building; energy simulation; microclimate simulation

1 . Introduction

Building energy consumption is one of the three main energy consumption domains including industry and transportation, accounting for approximately 20 % of China's total primary energy in 2018 (Tsinghua University, 2020). One potential way to reduce building energy consumption corresponds to decisions made during the design phase, which can be accomplished by dynamic building energy simulation (DBES) tools. The simulation results of a building's energy consumption is closely related to the accuracy of the weather file comprising 8 760 hours of various climatic parameters such as air temperature and solar radiation (Tsoka et al., 2018). In present DBES tools, the mostly used weather file format is the Typical Meteorological Year (TMY) format (Hall et al., 1978), which consists of twelve Typical Meteorological Months (TMM) from the past decades (Tsoka et al., 2018). These data usually come from meteorological stations located in the rural zones (e.g. the airport), which have a very different morphological form compared to the urban areas composed of urban settlements.

China is moving towards urbanisation and this process will last for decades (Wei et al., 2016). During this process, urban settlements are formed by replacing natural surroundings by urban environments. For example, the ground surface is altered to more hard materials such as concrete and asphalt and the area of vegetation is sharply reduced (Maheshwari et al., 2020). This leads to unique microclimates in the urban areas. Urban microclimate can be defined as the local climate observed in urban areas, which can be significantly different from the climate of surrounding rural areas (Toparlar et al., 2018). Urban microclimate involves the local climate characteristics between the near-ground atmosphere and the topsoil in a relatively small space, including temperature, solar radiation, wind, humidity, etc. (Li

et al., 2014). The difference between urban microclimate and rural climate might bring potential simulation errors if TMY weather file is directly used in an urban building' energy performance. To avoid this, it is essential to take the microclimate's effects into account in DBES.

The urban heat island (UHI) effect is a well-known phenomenon among the microclimate features. It describes the phenomenon that air temperature in urban areas is higher than the surrounding rural areas. It is observed in many urban areas regardless the size and location (Imhoff et al., 2010 ; Li et al., 2018 ; Li et al., 2017 ; Oke, 1982 ; Santamouris, 2015 ; Yang et al., 2020 ; Zhou et al., 2017). It can be quantitatively described by the urban heat island intensity (UHII) which is the urban air temperature minus the rural air temperature (Yang et al., 2020). Occasionally, the urban air temperature can be lower than the rural air temperature, which is called the urban cool island (UCI) effect, and the temperature difference is the urban cool island intensity (UCII). Air temperature is one of the most important factors as it directly drives the operation of cooling/heating system and influences the corresponding building cooling and heating energy consumption (Li et al., 2019). Many studies reported that the UHI effect increases the cooling energy consumption and decreases the heating energy consumption (Li et al., 2019 ; Lowe, 2016 ; Skelhorn et al., 2016 ; Sun and Augenbroe, 2014). A weather input file considering the UHI effects can yield a more accurate result.

Li et al. (2019) summarised the procedure in evaluating UHI impacts on building energy consumption, which includes three steps: (1) preparing two temperature datasets with and without UHI effect; (2) simulating/estimating building energy consumption respectively using two temperature datasets; and (3) evaluating the impacts of UHI on building energy consumption by comparing two results. The urban temperatures are mainly obtained by measurements or simulation. This paper focuses on the simulation of UHI, because as abovementioned normally the weather files in DBES are TMY format, reflecting the representative climates during a long period. On the contrary measurements, can only record the climate in a short time which might not be representative. This problem can be avoided by simulation method. Microclimate simulation tools (e.g. ENVI-met) can be used to obtain the UHI effects. However, the calculation time is quite long for a standard PC (e.g. nearly 24 hours to simulate one day in our case), so that it is not possible to obtain the hourly microclimate data for the whole year in a timely manner, especially if the energy performance optimisation of a building or a block is needed in the design phase. A method for the hourly microclimate parameters generation could be beneficial. Besides, the newly built buildings are usually high-rise and dense in China. Instead of low-rise buildings, few researches focus on the effect of UHI on a high-rise building in a dense building region. Normally, one air temperature is used for the whole building in DBES, neglecting the temperature variation along height and orientation. This might bring simulation errors for a high-rise building, especially where the UHI effect occurs.

This paper aims at investigating these two questions. Firstly, a site-specific weather file generation method is proposed to account for hourly UHI effect for a TMY weather file, avoiding long simulation time. Secondly, the coupling methodology of microclimate simulation tool and DBES tool is presented to perform a more accurate simulation of the building energy performance under the UHI effect. Finally, the methods are applied to a high-rise residential building in Wuhan (China) to quantitatively evaluate the effects of UHI on the energy performance.

2 . Methodology

2.1 Site-specific weather file generation method

In this paper, the microclimate's effect is evaluated by ENVI-met, which is a three-dimensional (3D) numerical model initially developed by Bruse and Fleer (1998) to analyse microclimates through the fundamental laws of fluids and thermodynamics. The interactions between buildings, soil, vegetation and atmosphere can be simulated with a typical spatial resolution between 0.5 m and 10 m and a

timestep of 1 - 10 s. Every single plant and every urban structure can explicitly be simulated, making ENVI-met the perfect tool for urban planners, architects and urban climatologists who want to simulate the meteorological components of the urban environment (Huttner, 2012). This model has been validated by several studies (Ayyad and Sharples, 2019 ; Elwy et al., 2018 ; López-Cabeza et al., 2018 ; Sharmin and Steemers, 2017 ; Tsoka et al., 2018 ; Yang et al., 2013) for different cities with different microclimate conditions. COMFIE (Peuportier and Blanc-Sommereux, 1990) is a multizone DBES model based on the finite volume method and modal analysis. It has been validated in several projects (Peuportier, 1993 ; Peuportier, 2005 ; Brun et al., 2009 ; Recht et al., 2014 ; Spitz, 2012), including in Wuhan (China) context (Pei, 2015).

As mentioned in the introduction, it is not possible to obtain the hourly microclimate effects for one year in ENVI-met with a standard PC in a reasonable calculation time. Therefore, the key point for the association of the DBES simulation tool and the microclimate tool is to propose a method which can generate a "site-specific weather file" containing the hourly microclimate's effects appropriately in reasonable simulation time. Since simulations for the evaluation of the microclimatic conditions are mainly conducted for a diurnal cycle, a specific day has to be defined for the analysis (Tsoka et al., 2018). This study focuses on the UHI effect, which is directly related to the ambient temperature, it is logic to select the representative day based on the air temperature. To find a compromise between the simulation time and accuracy, one representative day is chosen for each season: extreme hot/cold days in summer/winter (in order to obtain potential largest/smallest UHII) and average temperature days in spring/autumn (in order to obtain reasonable interpolation between largest and smallest UHII).

The reference typical weather file for DBES in COMFIE in this paper is an EPW format file downloaded from the website of EnergyPlus (EnergyPlus, 2021). It is a TMY format which can appropriately represent the typical meteorological conditions in the past decades. The reason why EPW file was chosen is that it can be directly and easily imported in the full-forcing function in ENVI-met to generate the forcing file for microclimate simulation. The other reason is that this file also records the extreme air temperature weeks in summer and winter and the average air temperature weeks for all four seasons, which is convenient to analyse the representative days of the four seasons. It should be noted that, if not especially indicated, spring refers to March, April and May; summer refers to June, July and August; autumn refers to September, October and November; winter refers to December, January and February.

To be more detailed, the proposed site-specific weather file generation method considering the local microclimate consists of four steps, as shown in Figure 1 (Matlab was used in steps 1, 3 and 4):

1. One representative day of the representative week (extreme hot/cold week for summer/winter and average week for spring/autumn, which are directly given in EPW file) of each season is chosen based on: the day with the hourly temperature closest to the average hourly temperature of the week. It should be noted that it is not the extreame hot/cold day in extreme hot/cold week for summer/winter, in order to be more presentaitve. These four representative days can be abbreviated to ex-summer, ex-winter, av-spring and av- autumn;
2. Then these four representative days are simulated in ENVI-met to obtain the local microclimate parameters and the UHIIs;
3. The hourly UHIIs are obtained with linear interpolation for 24 hours between each two representative days;
4. The air temperature of the site-specific weather file is generated by adding the hourly UHII to the original EPW file.

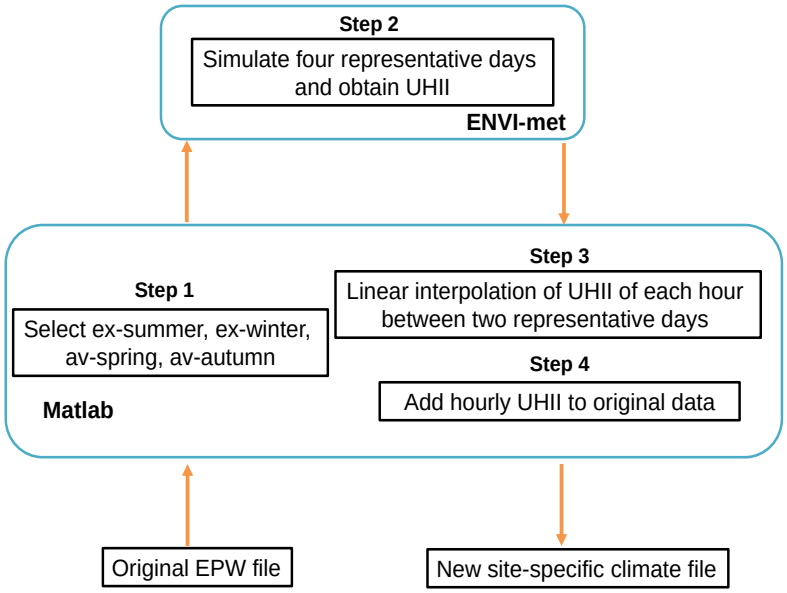

Figure 1: Algorithm of the proposed method to generate the site-specific weather file

In step 1, in order to determine the representative day of the representative week of each season, the average temperature of i^{th} hour $T_{av,i}$ of the representative week is firstly to be identified:

$$T_{av,i} = \frac{\sum_{j=1}^{7} T_i^j}{7} \quad i = 1 \dots 24 \tag{1}$$

where T_i^j is temperature of the i^{th} hour of the j^{th} day in the representative week.

The root mean square error (RMSE) and the mean absolute error (MAE) of each day for the 24 hours are calculated by:

$$RMSE_j = \frac{\sqrt{\sum_{i=1}^{24}(T_i^j - T_{av,i})^2}}{24} \tag{2}$$

$$MAE_j = \frac{\sum_{i=1}^{24}\left|T_i^j - T_{av,i}\right|}{24} \tag{3}$$

The day with the smallest RMSE is chosen as the representative day of each season; if RMSE is similar, the day with smallest MAE is selected.

In step 3, knowing the four representative days, the UHII of the i^{th} hour of the j^{th} day in the whole year can be calculated by linear interpolation:

$$\mathrm{UHII}_i^j = \frac{\mathrm{UHII}_i^{j_{re2}} - \mathrm{UHII}_i^{j_{re1}}}{j_{re2} - j_{re1}}(j - j_{re1}) + \mathrm{UHII}_i^{j_{re1}} \tag{4}$$

where j_{re1} and j_{re2} are the day numbers of the 1st and 2nd representative day.

It should be noted that the linear interpolation between two representative days to obtain the hourly UHII for the whole year is a highly simplified assumption. The hourly variation of UHII in cities is much more complex due to enormous factors such as complicated urban planning, various constructions, vegetation and climate conditions. The main aim of this study is to identify the UHI effect on the building energy consumptions for a long period (usually one year), rather than accurately estimate the UHI variation of one day. It mainly relies on the estimation of a general UHI feature, so there is a certain tolerance on the biases of hourly UHII (Yang et al., 2019).

2.2 Coupling microclimate simulation tool with DBES tool

The coupling of a microclimate tool and a DBES tool are classified into one-way coupling and double-way coupling (Lauzet et al., 2019). The double-way coupling method considers the effect of the microclimate on the building, as well as the effect of the building on the microclimate (e.g. the anthropogenic emissions released outside due to air-conditioning or heating systems such as heat pumps), which is more realistic, but more complex. It requires the microclimate tools to deal with such heat sources, and needs user parameters input.

In this paper, the coupling of ENVI-met and COMFIE is a one-way coupling, meaning the simulation results of ENVI-met are transferred to COMFIE but without feedback. The key point in the coupling of a microclimate simulation tool and a DBES tool is modifying the weather input file from the original one (e.g. the meteorological data from rural stations) to the new one (which considers the urban microclimate). In COMFIE, a building is modelled by defining thermal zones according to the orientations and heights. An identical temperature profile is used for the whole building, regardless of its height and zone orientation. As mentioned in the introduction, this might bring simulation errors for a high-rise building in a dense block where the UHI effect occurs.

The coupling method proposed in this paper considers the air temperature variation with height and orientation, based on the microclimate simulation results. The main 3D model in ENVI-met (e.g. a disctrict and its soil and atmosphere) is divided into a rectangular grid consists of $I \times J \times K$ cells with dimensions $\Delta x \times \Delta y \times \Delta z$. Buildings, vegetation and the digital elevation model are constricted to this rectangular grid. This means that a cell is either fully occupied by one of these obstacles or not at all. On the horizontal surface, Δx and Δy (usually from 0.5 m to 10 m) are constant for all the cells. On the vertical direction, Δz can be defined from four types (Yang, 2012), as shown in Figure 2. Generally, the cell close to the ground surface should have a smaller dimension, in order to have a more accurate simulation of the interactions between the ground and the atmosphere.

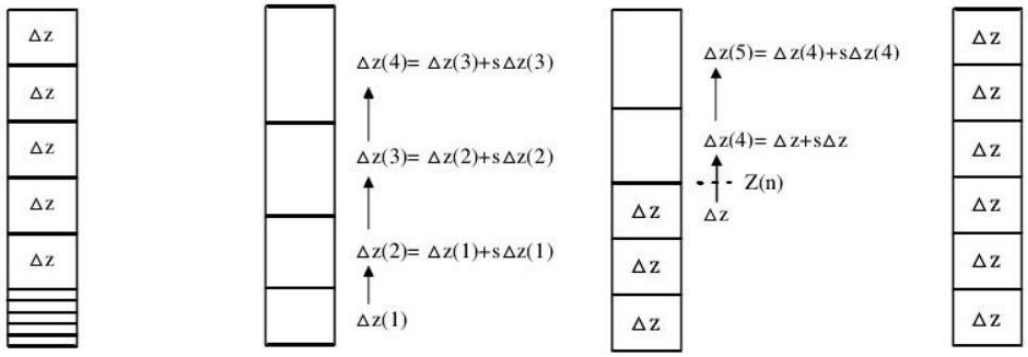

(a) Constant Δz (bottom cell is dividied into 5 subcells)

(b) Telescoping Δz

(c) Telescoping Δz (telescope from n^{th} cell)

(d) Constant Δz

Figure 2: Four types of vertical grid in ENVI-met (Yang, 2012)

The temperature profiles of four orientations (north, south, west and east) along N_h different heights are generated from the microclimate simulation tool ENVI-met. The value of N_h should respect the thermal zone definition regarding the height and in DBES tool and the definition of Δz in ENVI-met. This will be described in detail in section 3.3. The temperature profiles are inputted in the weather generation tool Meteocalc (which is integrated in COMFIE) and the $4 \times N_h$ corresponding site-specific

weather files are generated. Then, the simulation run $4 \times N_h$ times in COMFIE to obtain the accurate simulation results for each thermal zone. The whole coupling method is shown in Figure 3.

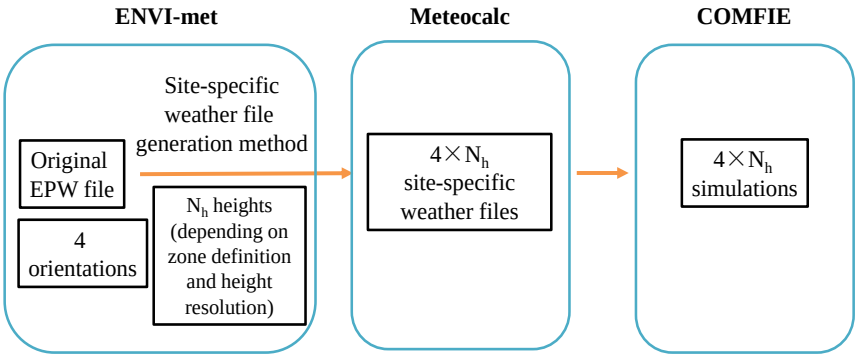

Figure 3: Method of coupling microclimate tool with the DBES tool

3 . Case study

3.1 Basic information

The studied case is located in Wuhan, capital city of Hubei Province, China. Its topography is dominated by relatively flat land between 22 m and 27 m above sea level except the hilly areas sporadically distributed in suburban districts. Water body occupies a high percentage (>20 %) of its territory. Wuhan's climate is humid subtropical with abundant rainfall and four distinctive seasons. Spring and autumn are generally mild, summer is hot and humid and winter is cold and dry.

The simulated high-rise building is unit 2 of building #2 (#2.2) in Haishan Jingu (HSJG) block. HSJG consists of one office building (#1) and three residential buildings (#2, #3 and #4). It is situated at the intersection between Zhongbei road and Donghu Xi road of Wuchang District, with a latitude of 30°32' North and a longitude of 114°20' East. This area is a business and commercial centre, mixed with many recently built high-rise office, commercial and residential buildings and old buildings, as shown in Figure 4 (a). This area faces south by east with an angle of 20°. The overall plan is shown in Figure 4 (b). The studied building #2.2 consists of 34 floors with an average height 3 m for each floor. The net floor area of the building is around 12 500 m^2.

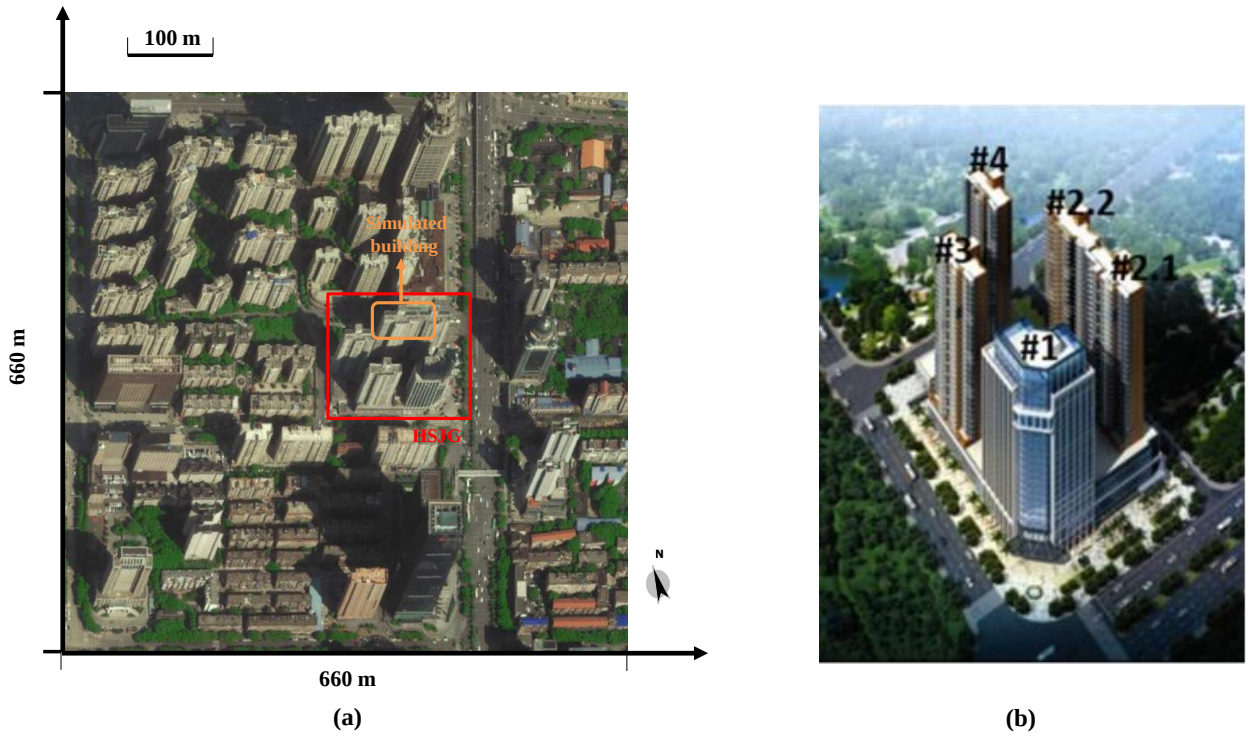

Figure 4: (a) Simulated area in ENVI-met and (b) HSJG block

3.2 Microclimate simulation configuration

3.2.1 Representative days selection

The EPW file downloaded from EnergyPlus website directly indicates the four representative weeks of the four seasons, as shown in Table 1. Using the site-specific weather file generation method, the representative day of each season was selected for the microclimate simulation. The day of each week with the smallest RMSE was chosen as the representative day for each season. The results are shown in Table 1. The microclimate simulation has better accuracy with a buffering time, thus an extra day ahead (48 hours in total) was used to obtain more precise simulation results.

It should be noted that instead of a normal air temperature (e.g. in EPW file), the air temperature in ENVI-met, $T_{\text{air,pot}}$, is the potential temperature. It can be converted from atmosphere pressure and normal temperature with the following equation (5):

$$T_{\text{air,pot}} = T_{\text{air}}^{\text{abs}}\left(\frac{P_0}{P}\right)^{0.286} \quad \textbf{(5)}$$

where $T_{\text{air}}^{\text{abs}}$ is the absolute normal air temperature (K), P_0 is the reference pressure (100 000 Pa in ENVI-met) and P is the atmosphere pressure (Pa).

Table 1: Representative days selection of each season

Season	Representative week	Representative day	Abbreviation	RMSE (°C)	MAE (°C)
Summer Extreme hot	Aug 05-11	Aug 09	Ex-summer	0.82	0.76
Winter Extreme cold	Jan 01-07	Jan 04	Ex-winter	1.11	0.90
Spring Average temperature	May 27-Jun 02	Jun 02 (date is in June, but represents spring)	Av-spring	1.48	1.19
Autumn Average temperature	Nov 26-Dec 02	Nov 30	Av- autumn	1.25	1.02

3.2.2 Simulation configuration

Locating the studied building approximately in the centre, the total area for microclimate simulation is a region of 660 m × 660 m, as shown in Figure 4 (a). Although it is very difficult to obtain the detailed surroundings information, it is still possible to get a rough picture of the surroundings including the heights of the buildings, the green areas and the roads by using Google Map and Google Earth. This information allows one to use ENVI-met to evaluate the site-specific climatic conditions. If detailed data of the surroundings can be obtained, a more accurate simulation can be performed. Accounting for the calculation speed and the model accuracy, 110 × 110 × 19 cells were used in this study, with the resolution of 6 m in the horizontal directions. In the vertical direction, the resolution of one cell is 6 m below 30 m (the first 5 cells) and afterwards the height of cell $n + 1$ is the height of cell n multiplied by 1.25 (n being the level of the cell from 6 to 19), as shown in Figure 2 (c). Besides, 8 empty cells were set at each border to increase the stability and accuracy of the simulation ("nesting area").

The ground in the simulated area mainly contains four types of ground profiles: the brick road, the concrete field, the green field and the asphalt concrete road. The compositions of the ground profiles in ENVI-met are listed in Table 2 (Yang et al., 2013).

Table 2: Composition and depth in the ground profiles in ENVI-met

Brick road	Concrete field	Green field	Asphalt concrete road
Brick: 0~3 cm	Concrete: 0~20 cm	Sandy loam: 0~40 cm	Asphalt: 0~10 cm
Concrete: 4~20 cm	Sand: 21~ 30 cm	Loam: 41~450 cm	Sand: 11~40 cm
Sand: 21~30 cm	Loam: 31~450 cm		Loam: 41~450 cm
Loam: 31~450 cm			

The initial temperature and the relative humidity for the four layers of the soil are also needed: upper layer (0-20 cm), middle layer (20-50 cm), deep layer (50-200 cm) and bedrock layer (below 200 cm). Assuming the soil is semi-infinite and with unique physical properties, the soil temperatures were estimated by the method from Thiers (2008). The corresponding soil relative humidities of the four layers in ENVI-met were calculated from Wu et al. (2017). They are summarised in Table 3.

Table 3: Soil temperature and relative soil humidity of each soil layer in ENVI-met

	Av-spring	Ex-summer	Av- autumn	Ex-winter
Upper layer (0-20 cm)	26°C/77 %	33.51°C/85 %	12.33°C/84 %	6.16°C/80.5 %
Middle layer (20-50 cm)	24.66°C/80.5 %	32.57°C/81 %	13.66°C/83 %	7.53°C/83 %
Deep layer (50-200 cm)	21.07°C/82 %	29.30°C/79 %	17.20°C/81 %	11.65°C/84 %
Bedrock layer (below 200 cm)	19°C/82 %	19°C/79 %	19°C/81 %	19°C/84 %

It should be noted that the density of the plants' leaves vary with the season in the simulation. Considering the aim of ENVI-met simulation is to obtain the outdoor air temperature, instead of the indoor thermal comfort or other parameters concerning the building envelope, the building's envelope configuration is not as important as other configurations, especially in a "one-way" coupling method. Therefore, the envelopes of all the buildings are set to be identical, as shown in Table 4.

Table 4: Wall configuration of the buildings in ENVI-met

External wall	**Roof**
Ceramic tile 1 cm	Ceramic tile 1 cm
Insulation mortar 4 cm	Extruded Polystyrene Board (XPS) 4 cm
Aerated concrete block 20 cm	Concrete (C10) 20 cm

Receptors are the selected points inside the model area, where processes in the atmosphere and the soil are monitored in detail. They record the detailed simulation results for each height of the node on the vertical axis. As introduced in section 2.2, in order to analyse the effects of the orientation on the building's energy performance, four receptors located at 3 m away from the simulated building's four facades were used: North (N), West (W), South (S) and East (E). The whole 3D model and the receptors are shown in Figure 5.

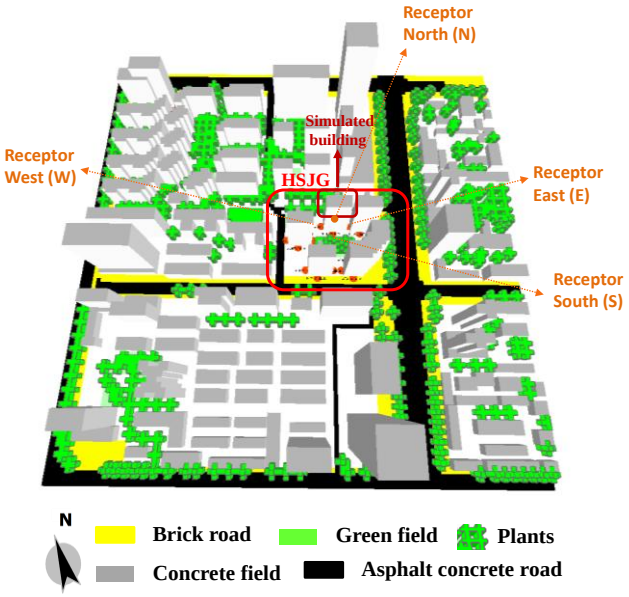

Figure 5: 3D model of the simulated area and four receptors in ENVI-met

3.3 DBES configuration

According to the Chinese building energy standard (MOHURD, 2010), the heating and cooling thermostat setpoints are 18 °C and 26 °C for the whole year. The natural ventilation is 1 ach (air change per hour) because residents in Wuhan prefer opening windows for ventilation; an additional 0.2 ach accounts for the infiltration ventilation. The internal heat gain is 4.3 W/m^2 for all the time. The occupancy is 0.02 person/m^2 from 8h00 to 17h00 from Monday to Friday and the rest of the time, it is 0.04 person/m^2.

In the studied building, each floor consists of four apartments named A, B, C, D (from west to east) and aisle. The 15th floor plan of building #2.2 is shown in Figure 6 as an example, and the plan of each floor is similar. The areas surrounded by dotted lines are the balconies functioning as integrated shadings in the simulation. Windows and doors are shown in blue and brown lines on the walls correspondingly. The building was divided into 17 thermal zones based on the height and orientation (see Table 6). Apartments A and D consist of the north zone and apartments B and C consist of the south zone for one or several floors. It should be noted that the apartment C on the 15th floor was un exception, which contains three zones, because experiments were conducted in the previous work (Pei, 2015) in this apartment and a more detailed zone definition was required. The studied case and its zones are shown in Figure 7.

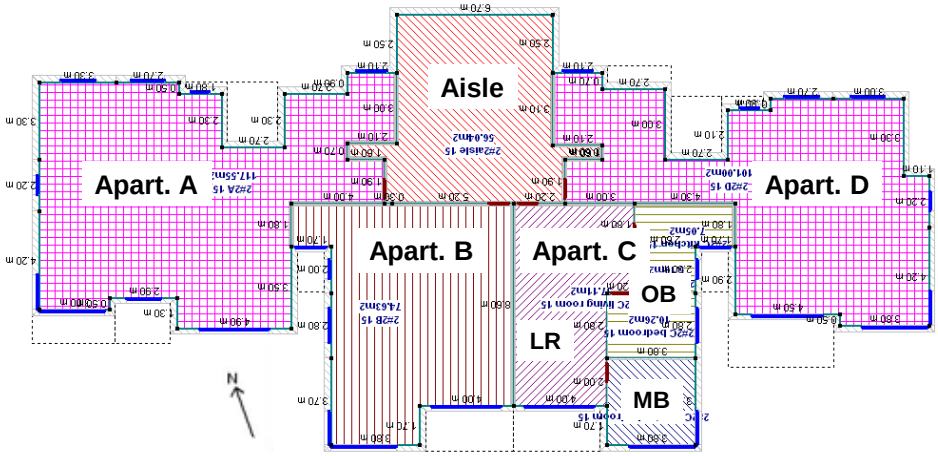

Figure 6: 15th floor plan of the case study

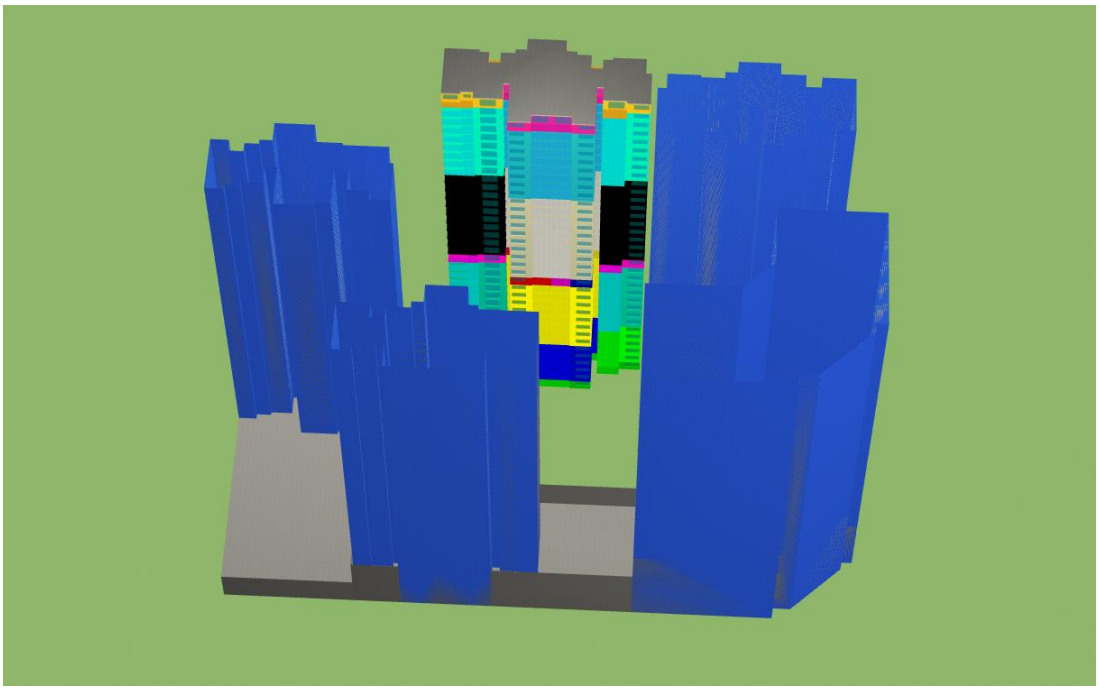

Figure 7: South view of HSJG and its zones in COMFIE

Combining the zone definition and the height of ENVI-met cells, six different heights were chosen for the DBES weather file generation. Taking level 2 – 6 as an example, its height is from 6 m to 18 m. The vertical cells 2 and 3 in ENVI-met record the air temperatures at 9 m and 15 m, which are located between level 2 – 6. Thus we use the average of the air temperatures at 9 m and 15 m in ENVI-met to generate the weather input file for level 2 – 6 (which contains two zones). Considering four orientations (N, W, S, E) and 6 heights (from #1 to #6), 24 DBES weather files were generated as inputs for the energy simulation, as illustrated in Table 5. The abbreviation of one file can be expressed by orientation#height number (e.g. N#1).

Table 5: The height of weather file for building energy simulation

Building level	**Level height**	**Weather file abbreviation of 4 orientations at each height**	**Height of the weather file by averaging the heights of vertical cells in ENVI-met**
1	3 m	N#1, W#1, S#1, E#1	3 m (cell 1)
2 – 6	6 – 18 m	N#2, W#2, S#2, E#2	(9 m (cell 2)+ 15 m (cell 3)) / 2 = 12 m
7 – 14	21 – 42 m	N#3, W#3, S#3, E#3	(21 m (cell 4) + 27 m (cell 5) + 33.75 m (cell 6) + 42.19 m (cell 7)) / 4 = 31 m
15 – 25	45 – 75 m	N#4, W#4, S#4, E#4	(52.73 m (cell 8) + 65.92 m (cell 9)) / 2 = 59.3 m
26 – 33	78 – 99 m	N#5, W#5, S#5, E#5	82.4 m (cell 10)
34	102 m	N#6, W#6, S#6, E#6	103 m

Based on the zone definition (Figure 6), the south zones are mainly affected by the air in south, and the north zones are surrounded by the air in all the four orientations. To perform a precise energy performance simulation, the loads of each zone are calculated using the meteorological files according to the orientation and height, as shown in Table 6. The heating/cooling load of the north is the average

of the corresponding simulation results from the four weather files of N, S, W and E. For the south zone, it is directly the simulation results from weather file S.

Table 6: Meteorological files to calculate the energy load of each zone

Zone number	Zone name	Weather file
1	floor 1	(N#1+S#1+W#1+E#1)/4
2	aisle	-
3	floor 2-6 north	(N#2+S#2+W#2+E#2)/4
4	floor 2-6 south	S#2
5	floor 7-14 north	(N#3+S#3+W#3+E#3)/4
6	floor 7-14 south	S#3
7	floor 15 C-living room (15)	S#4
8	floor 15 C-master bedroom (15)	S#4
9	floor 15 C-other rooms (15)	S#4
10	floor 15 B	S#4
11	floor 15 north	(N#4+S#4+W#4+E#4)/4
12	floor 16-25 north	(N#4+S#4+W#4+E#4)/4
13	floor 16-25 south	S#4
14	floor 26-33 north	(N#5+S#5+W#5+E#5)/4
15	floor 26-33 south	S#5
16	floor 34 north	(N#6+S#6+W#6+E#6)/4
17	floor 34 south	S#6

4 . Results and discussion

4.1 Microclimate simulation results

Figure 8 to Figure 11 show the potential air temperature maps of the simulated region for the four representative days at the height of 3 m at 13h00 (av-spring and ex-summer) and 14h00 (av-autumn and ex-winter) when the maximum UHIIs are observed. The northeast region containing the asphalt road and the southwest region respectively show the highest and lowest UHI effect on all these four days. On ex-summer and av-autumn, the UHI effect is obvious along the north-south asphalt road; the north part has a stronger UHI effect. The temperature surrounding HSJG can vary over 1.5 °C on ex-summer, particularly higher on the side of the north-south asphalt road, but on other days the temperature difference is not very large (< 0.5 °C).

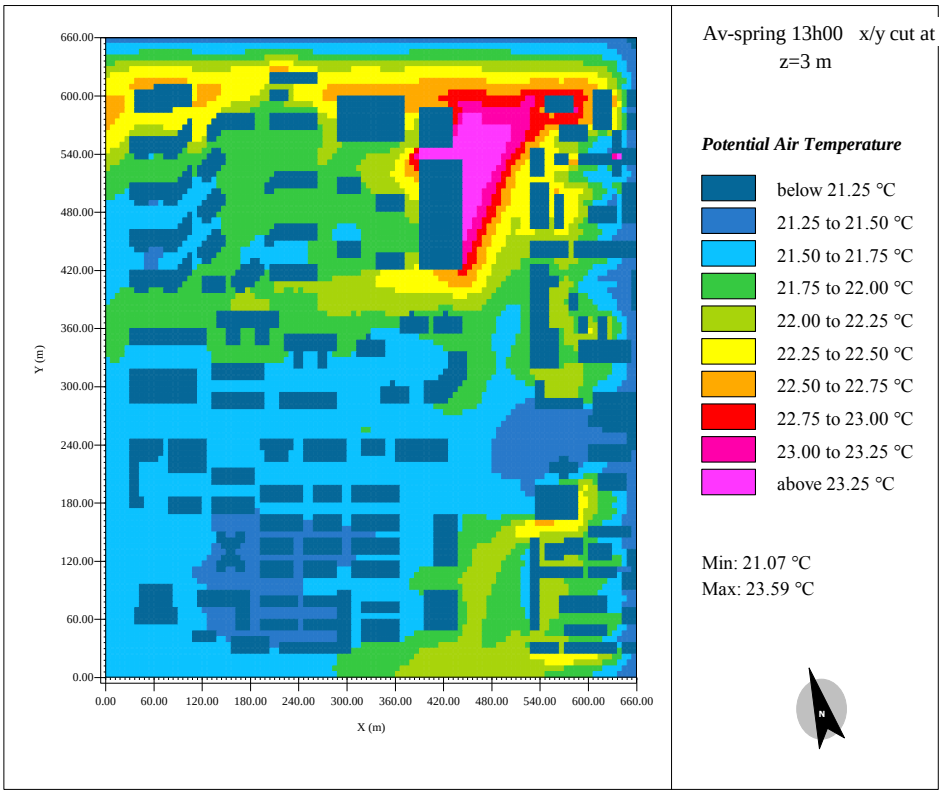

Figure 8: Potential temperature map of the simulated area for av-springat the height of 3 m

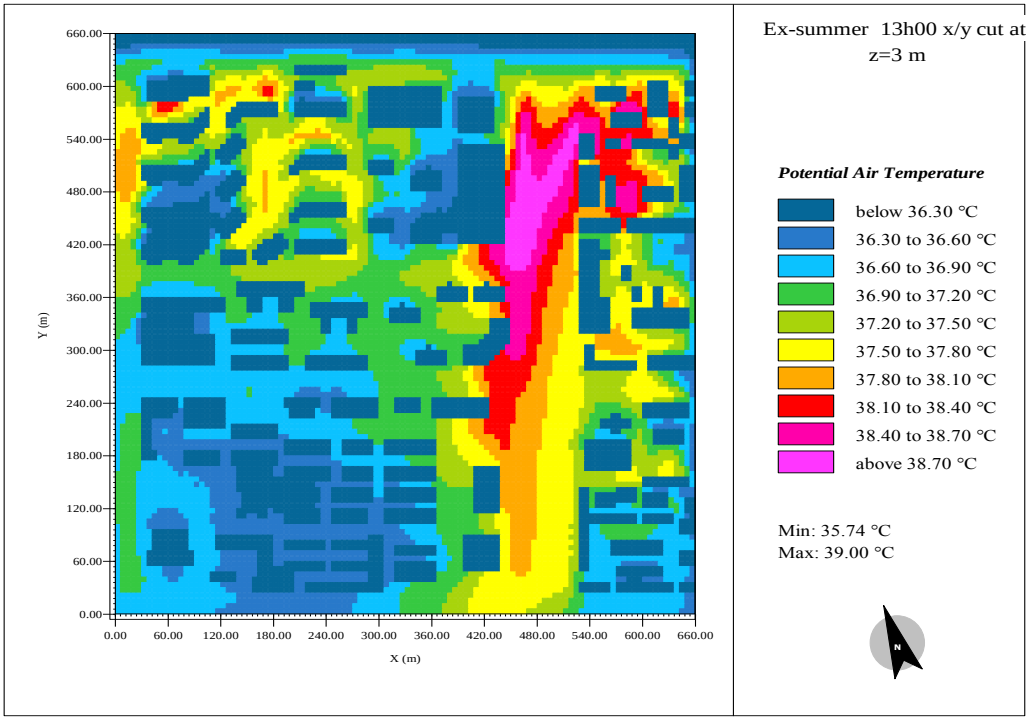

Figure 9: Potential temperature map of the simulated area for ex-summer at the height of 3 m

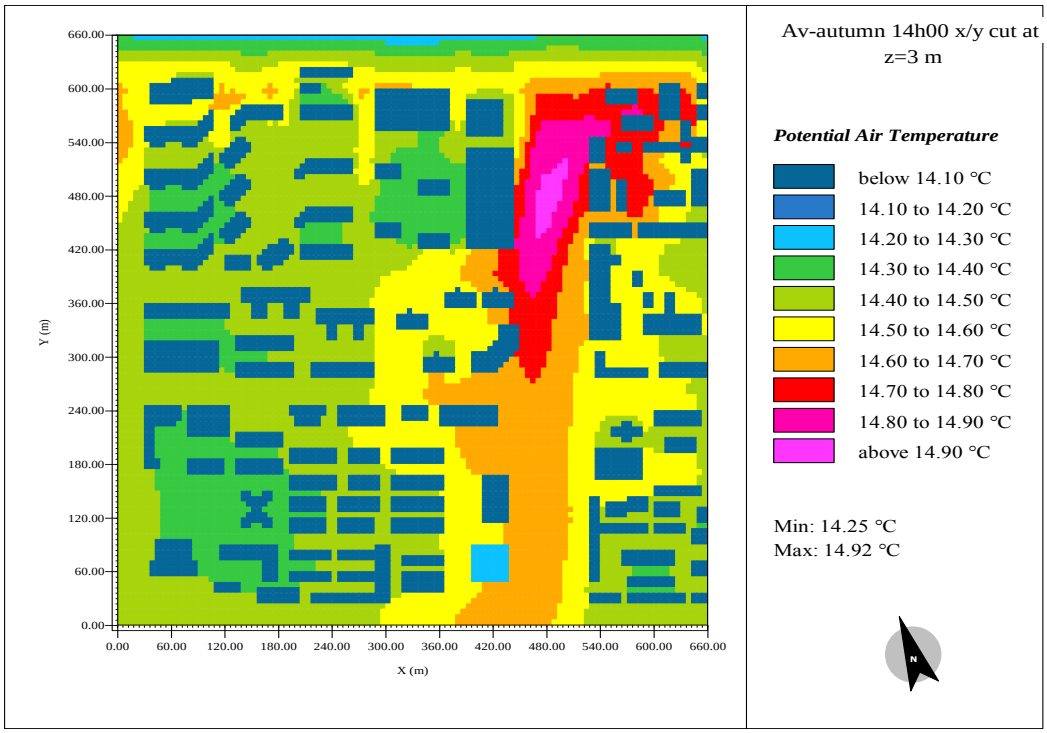

Figure 10: Potential temperature map of the simulated area for av-autumn at the height of 3 m

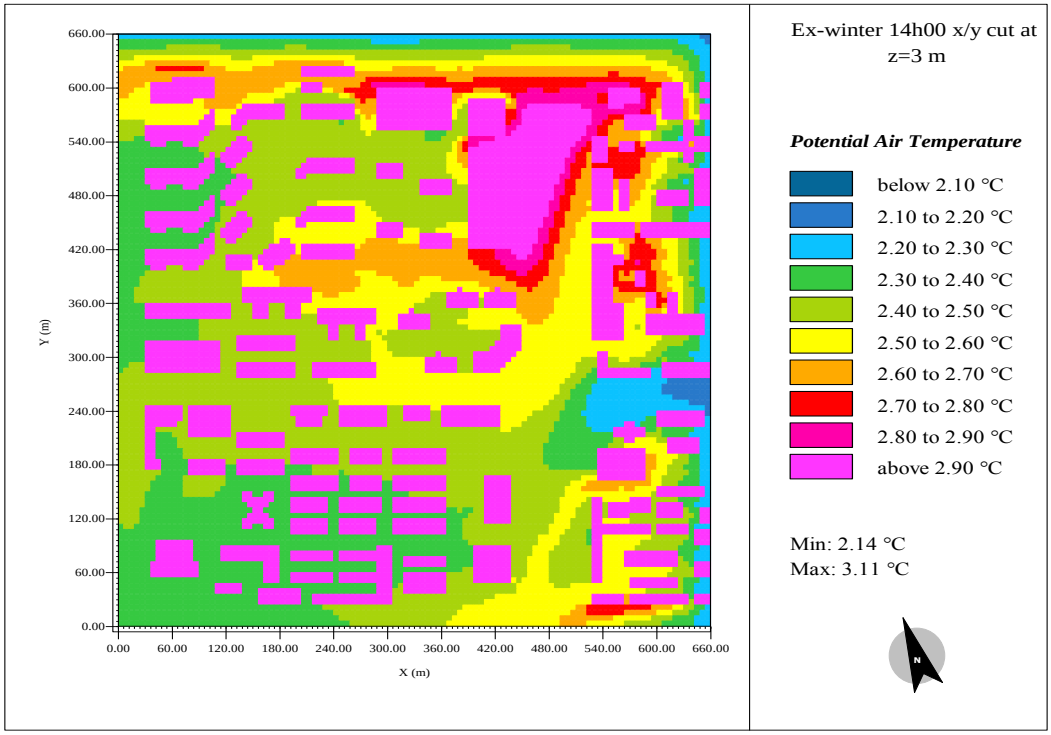

Figure 11: Potential temperature map of the simulated area for ex-winter at the height of 3 m

4.2 UHI results for the four representative days

The heat island effect can be quantitatively described by UHII:

$$\mathrm{UHII} = T_{\mathrm{air,ENVImet}} - T_{\mathrm{air,EPW}} \quad (6)$$

where $T_{\mathrm{air,ENVImet}}$ is the air temperature (°C) converted from the potential air temperature in ENVI-met simulation and $T_{\mathrm{air,EPW}}$ is the air temperature (°C) in EPW file.

The air temperature at the height of 3 m of the north receptor is shown in Figure 12. For av-spring, av-autumn and ex-winter, all the simulated air temperatures are higher than the input air temperatures. For ex-summer, in the morning there are several hours when the simulated air temperature is lower than the input air temperatures, meaning that there exists a "cool island" effect (Yang et al., 2016). However, the UHI effect starts to appear after 8h00, and it shows a maximal UHII of around 2.56 °C at 13h00. The hourly average UHII ($\mathrm{UHII_{av}}$) and maximal UHII ($\mathrm{UHII_{max}}$) of these representative days are listed in Table 7. It can be inferred that the largest $\mathrm{UHII_{max}}$ occurs on the extreme hot summer day and the smallest $\mathrm{UHII_{max}}$ occurs on the average autumn day. For the average UHII during one day, it is observed that ex-summer > av-spring > ex-winter > av-autumn.

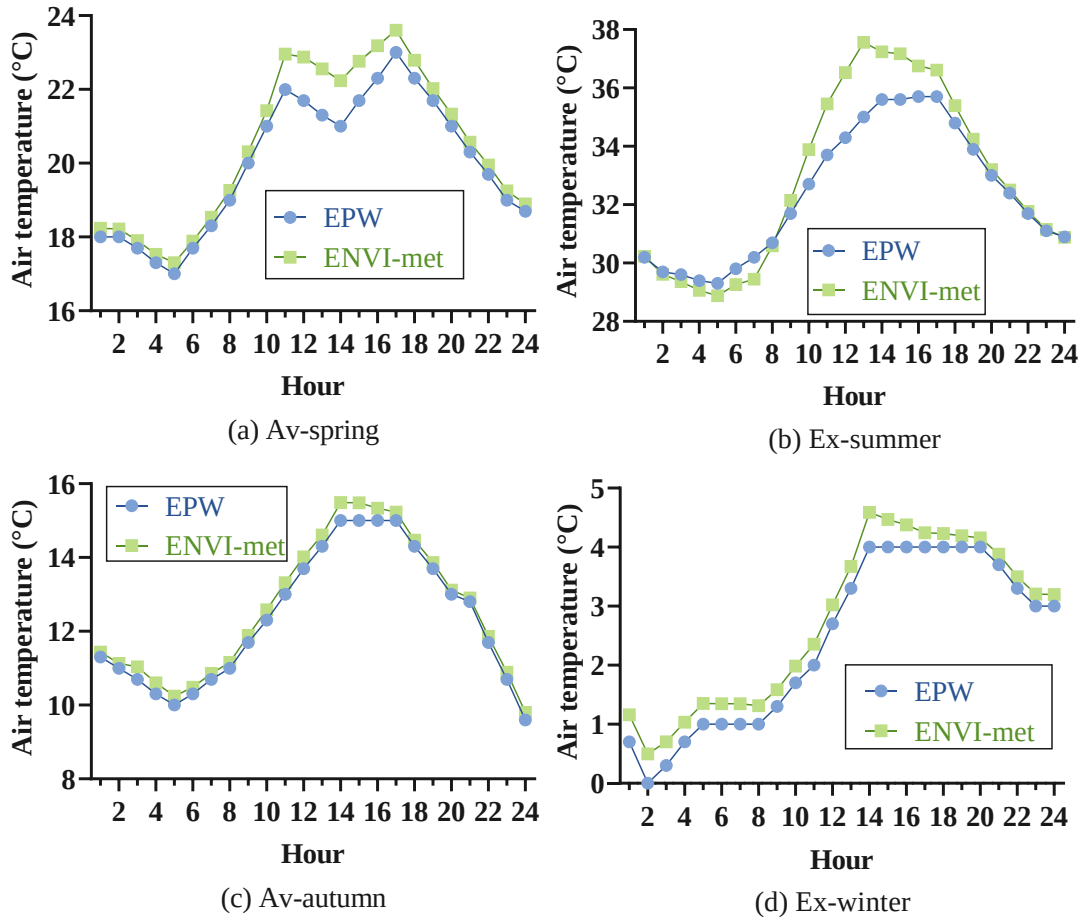

Figure 12: ENVI-met simulation results for the four representative days at the height of 3 m of the north receptor

Table 7: $UHII_{max}$ and $UHII_{av}$ at the height of 3 m of the north receptor

Representative day	$UHII_{max}$ (°C)	$UHII_{av}$ (°C)
Av-spring	1.26	0.50
Ex-summer	2.56	0.51
Av-autumn	0.49	0.24
Ex-winter	0.59	0.32

The air temperature along the height of the north receptor was investigated, as shown in Figure 13. In general, the air temperature decreases with the height. If the UHII is larger (e.g. 12h00 on ex-summer), the air temperature decreases more sharply. The air temperature at the height #1 (3 m) is 1.9 °C higher than at height #6 (103 m). The opposite trend is observed for the hours of UCI effect, e.g. 6h00 on ex-summer: the air temperature increases from 29.26 °C to 29.42 °C along the height. A more accurate building energy simulation should include the air temperature variation along the height.

The air temperatures of the four orientations at 3 m are compared in Figure 14. The temperature difference is negligible for av-autumn and ex-winter for the four receptors; however the difference can be more obvious from 10h00 to 14h00 on av-spring and from 8h00 to 16h00 on ex-summer. This means the orientation might potentially have a larger influence on the cooling load than on the heating load; it will be discussed in section 4.4.

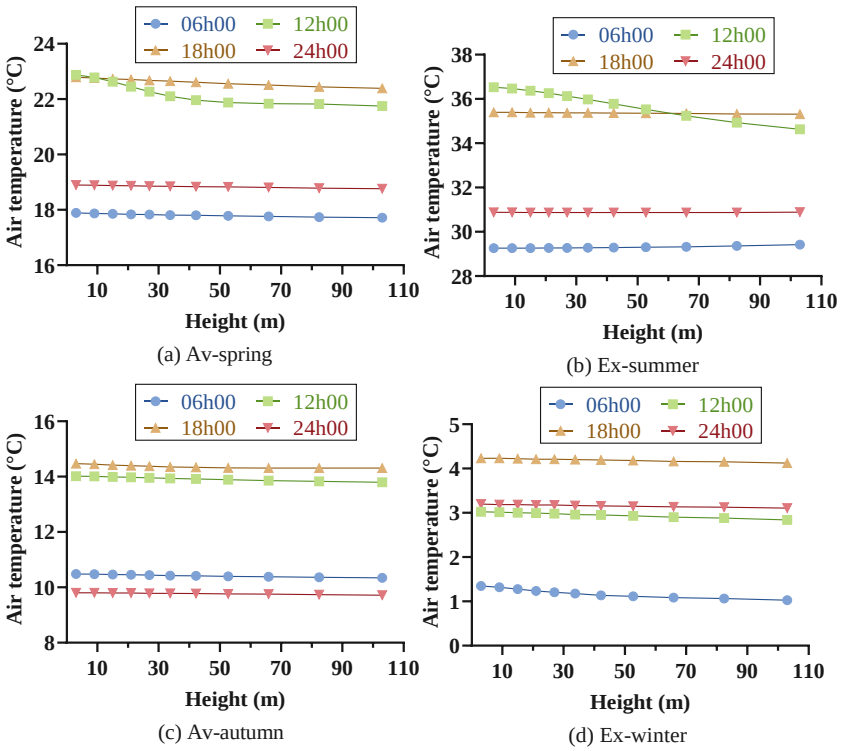

Figure 13: Air temperature evolution along height for four representative days of receptor N

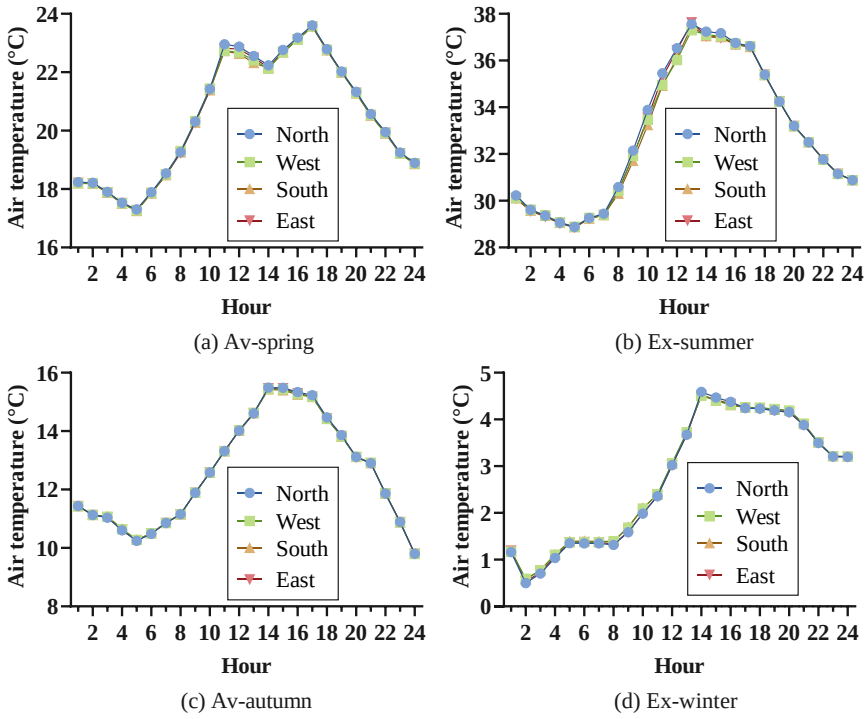

Figure 14: Air temperature of the four orientations at height #1 for the four representative days

4.3 Generated weather files for COMFIE

Applying the method illustrated in section 4.2, the meteorological files for building energy simulation were generated. The UHIIs at six different heights of four orientations were calculated and added to the original EPW file, meanwhile the other meteorological parameters were kept the same. In total 24 meteorological files taking into account the local microclimate effects were generated and were used to simulate the building's energy performance. The hourly temperature of N#1 is shown in Figure 15, compared to the original EPW. The yearly average UHII at the height of 3 m is estimated to be 0.45 °C (considering the average of four orientations).

The accumulations of hourly heat island or cool island intensity over TMY were calculated, namely urban heat island degree-hours (UHIdh) and urban cool island degree-hours (UCIdh) (Yang et al., 2018), as shown in Figure 16. UHIdh and UCIdh measure how much and for how long the air temperature at a site is higher and lower than the reference suburb, respectively. At height #1, the values of UHIdh are ranked in the following order: summer > spring > autumn > winter in the north and east; summer > spring > winter> autumn in the west and south. For the whole year, at height #1, the order of the number of UHIdh is N#1 (3 740 °C hours) > E#1 (3 490°C hours) > W#1 (3 420°C hours) > S#1 (3 320°C hours). At height #6, the order changes to: S#6 (922 °C hours) > E#6 (902°C hours) > W#6 (874°C hours) > N#6 (873 °C hours). UHIdh and UCIdh decrease with the height.

The ratio of UHI degree-hours to degree-hours of original EPW are presented in Figure 17, based on 18 °C for heating and 26 °C for cooling. This ratio indicates the potential of changing the heating/cooling load. For summer, N#1 has the largest ratio of around 22 %, which is almost 4 % larger than the smallest of S#1. For winter, the four orientations have similar ratios, indicating the heating load is not strongly influenced by the orientation. The ratio decreases with the height. At

height #6, the ratio drops below 1 % in winter and to around 6 % in summer. This indicates smaller effects are foreseen with the increase of the height.

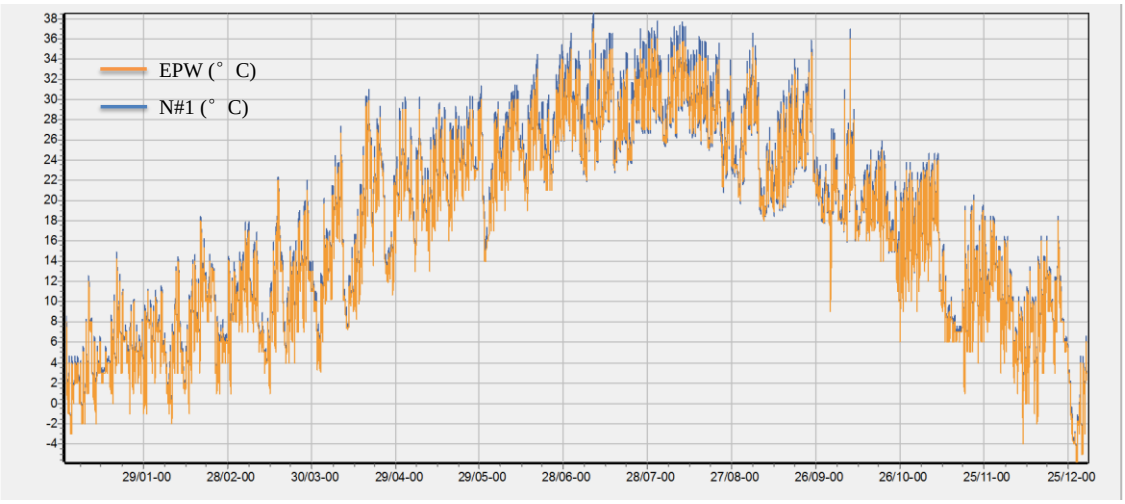

Figure 15: Air temperature of EPW and N#1

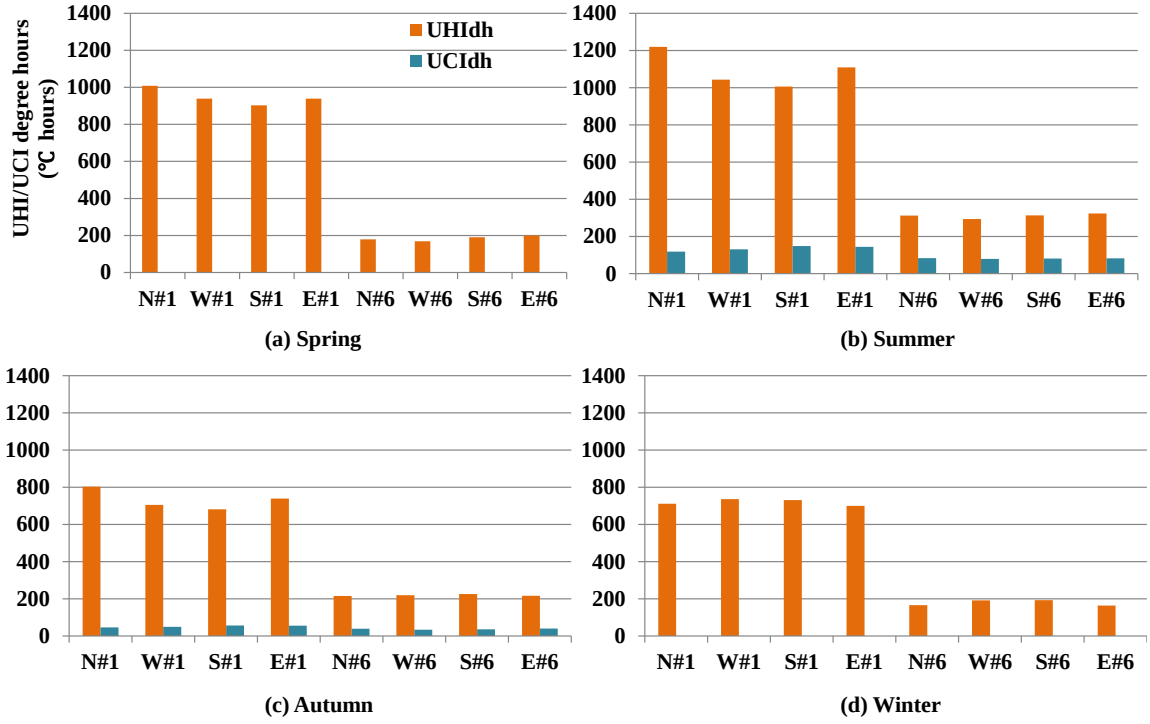

Figure 16: UHI/UCI degree-hours of four orientations at the height #1 and #6 for four seasons

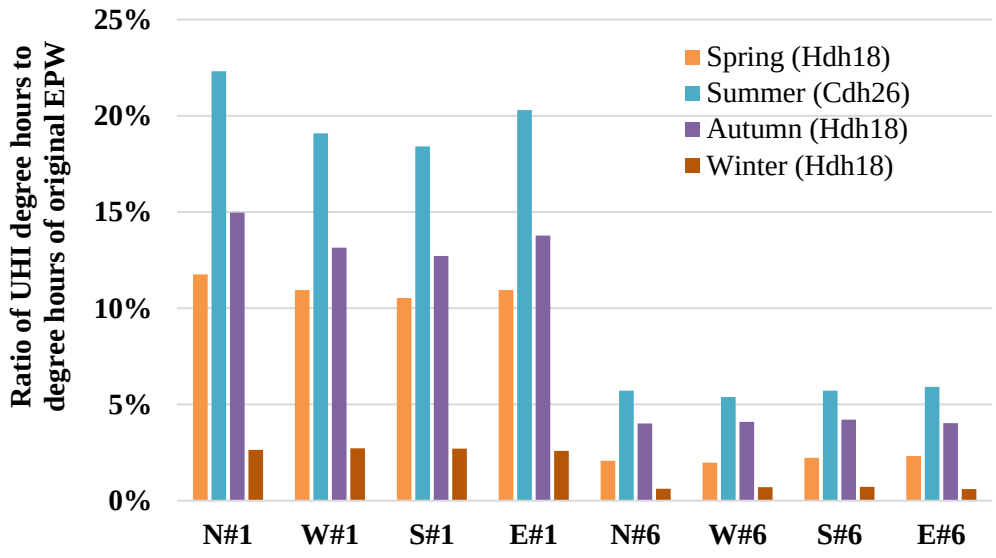

Figure 17: Ratio of UHI degree hours to degree hours of original EPW

4.4 Building energy simulation results

4.4.1 DBES with detailed microclimate data

Applying the proposed methods, the energy simulation results with detailed microclimate data were obtained: the total heating and cooling loads are 586 000 kWh (47.1 kWh/m^2) and 582 000 kWh (46.7 kWh/m^2), respectively. Since this simulation considers the air temperature variation with height and orientation, it can be regarded to be closer to the reality and it is used as a reference (legend "Ref" in Figures 18 and 19) to compare the differences of other simulation results such as the simulation with the original EPW file.

4.4.2 Impact of orientation and height

The simulation results of different meteorological files were compared including the original EPW and the reference simulation. Figure 18 shows the simulated annual loads of different orientation at a height of 3 m. Compared to the reference simulation, the simulation with EPW file shows a heating load 3.6 % larger, a cooling load 3.9 % smaller and a total energy load 0.2 % smaller. This is mainly due to the temperature from EPW file which is collected in the rural areas such as in the airport. The UHI effect reduces the heating load in winter and increases the cooling load in summer. At the height of 3 m, the orientation slightly affects the heating load, with a variation of only 0.2 % between north and east. The orientation has a larger influence on the cooling load. Compared to the reference simulation, the north shows a cooling load of 4.4 % larger, meanwhile the south only shows a 2.7 % increase. For the total energy load, the north has the biggest difference (1.1 %) and the south has the smallest (0.3 %). In general, the effect of orientation is not important in this case study, especially if the uncertainty is considered. However, the effect might be larger in some other cases. For example, the geometry and layout of the block and vegetation might influence the air temperature distribution (Huang and Li, 2017).

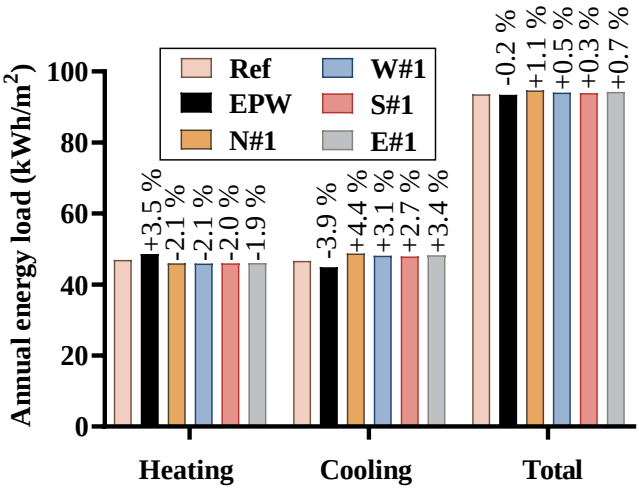

Figure 18: Energy loads for different orientations at the height #1

According to Figure 19, the air temperature drops along the height, yielding different energy loads. As abovementioned, the south orientation has a more accurate simulation result than the other orientations. The building energy simulation results of different heights for south are illustrated in Figure 19. It can be inferred that compared to the reference simulation, the difference in heating load increases from -2.0 % to +2.1 % and the difference in cooling load decreases from +2.7 % to -2.2 % with height. The height has a minor influence on the total load, with a maximal difference of ±0.3 %. Compared to EPW, the differences of heating load and cooling load can reach respectively -5.4 % and +6.9 % for S#1. Many studies only consider the UHI effect observed near the ground (e.g. S#1), neglecting its variation along height. This brings a larger difference than the reference simulation considering the variation along the height. The smallest differences are from the largest height S#6, with differences of -1.4 % and +1.8 %. It can be indicated that the microclimate's effects on the low-rise buildings is larger than the high-rise buildings. In this study, S#4 is the best representative meteorological file which can obtain the closest result compared to the reference simulation for both heating load (+0.4 %) and cooling load (-0.8 %). The simulation with the original EPW file did not consider the UHI effect, overestimating the heating load by 3.5 % and underestimating the cooling load by 3.9 %; however it can accurately predict the total energy load.

It should be noted that, in our case study, the heating and cooling loads are almost balanced, resulting in a minor difference in the total energy load due to the microclimate. However, its effect could be stronger in other climate zones where the difference between the heating and cooling loads is large.

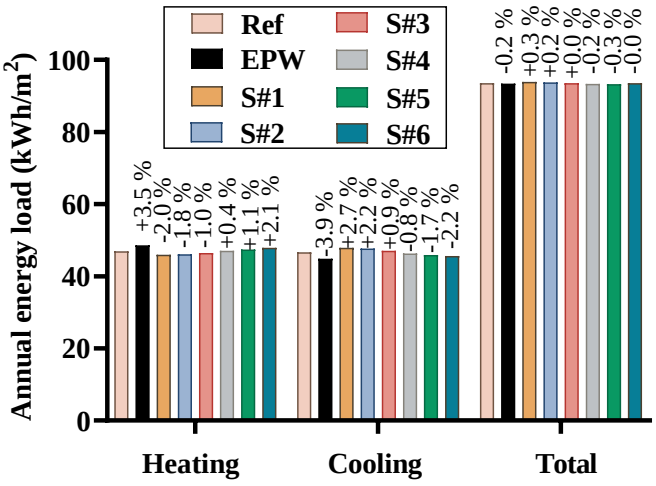

Figure 19: Annual loads of different heights for S orientation

4.5 Discussion

The method of generating the hourly UHII is based on the linear interpolation between four representative days in each season, which might not precisely evaluate the UHII for every hour. Although this is a good attempt to account for the local UHI effect on the building energy performance, a more accurate method generating the hourly UHII would be beneficial. Besides, measurements of the local climate parameters could be helpful to validate the simulation results. The energy performance of other uses of the building can also be investigated, such as the office buildings only operating in the daytime.

Although some studies, e.g. Chan (2011), reported a similar UHII measurement trend as Figure 12, in urban areas, a larger UHI effect is usually observed during the night period compared to the day time, which is contradictory to Figure 12. A longer buffering time of 3 days was used to investigate the possibility of improving the results. However the results still showed a limited heat island effect at night, which may be due to numerical approximation of ENVI-met. It would be useful to perform calculations again using a more powerful computer allowing more precise simulation options to be chosen.

This paper focuses on the influence of air temperature. Other site-specific climate parameters such as relative humidity, solar radiation, longwave radiation and wind affecting the building energy loads were not considered in this study, which is an interesting topic in future research.

This study only evaluates the effects of local microclimate on the energy consumption of the building. However there are other environmental impacts such as CO_2 emissions, human health and biodiversity. Moreover, the environmental impacts of electricity are different in winter and summer. Although the total energy consumption is almost identical, the variations in the heating and cooling loads might influence the environmental impacts. This is another interesting topic to be investigated.

5 . Conclusion

China is under rapid urbanisation. During this process, the urban environment is altered and shows different climate characteristics compared to the rural areas. The simulation results of a building's energy consumption highly depend on the accuracy of the weather file comprising 8 760 hours of various climatic parameters. In present DBES tools, the mostly used weather data usually come from

meteorological stations located in the peripheral zones, which cannot reflect the site-specific microclimate conditions, such as the UHI effect. This might lead to simulation errors.

This paper aims at accounting for the UHI effect in building energy simulation. A site-specific weather file generation method was proposed to generate new local weather files containing hourly UHI effect, by applying microclimate simulation tool ENVI-met as the microclimate simulation tool. This method selects four representative days which are simulated in ENVI-met to obtain the hourly UHII. Afterwards the corresponding hourly UHII of other days in one year are evaluated by linear interpolation. This method could avoid long simulation time which is a big challenge for building energy performance optimisation. The method of coupling ENVI-met with the DBES tool COMFIE was introduced as well. This method combines the thermal zone definition in COMFIE and the height resolution in ENVI-met, providing more precise weather data for each zone in DBES. By applying this method, instead of the same weather file for all the building zones, the air temperature variations along height and orientation are considered, yielding relatively more accurate simulation results, especially for high-rise buildings.

The methods were applied to a case study in Wuhan, China. A district area of 660 m × 660 m was modelled and the microclimate simulation was performed for four representative days by ENVI-met. The hourly UHII was obtained by applying the proposed method and a set of site-specific weather files considering UHI effect was generated for four orientations and six heights. The yearly average UHII at the height of 3 m was estimated to be 0.45 °C. The simulation using the original EPW file showed a heating load 3.5 % larger, a cooling load 3.9 % smaller, and a total energy load smaller 0.2 %, compared to the reference simulation. When only the weather file at the height of 3 m in the south was used, neglecting the variation of UHII along the height, the heating load decreased by 5.4 % and the cooling load increased by 6.9 % compared to the EPW file. The UHI's effects on the low-rise buildings are larger than on the high-rise buildings. The methods proposed in this paper can be used for a more precise application of urban building energy simulation accounting for the UHI effect. More climate features could be included in these methods in the future work.

Acknowledgement

The authors would like to thank the financial support by China Scholarship Council (CSC) and the Chair ParisTech VINCI Eco-design of buildings and infrastructure.

Reference

Ayyad, Y., and Sharples, S. (2019). *Envi-MET validation and sensitivity analysis using field measurements in a hot arid climate*. IOP Conference Series: Earth and Environmental Science *329*, DOI : 10.1088/1755-1315/329/1/012040, 012040 p.

Brun, A., Spitz, C., Wurtz, E., and Mora, L. (2009). *Behavioural comparison of some predictive tools used in a low-energy building*. (Glasgow, Scotland),.

Bruse, M., and Fleer, H. (1998). *Simulating surface–plant–air interactions inside urban environments with a three dimensional numerical model*. Environmental Modelling & Software *13*, DOI : 10.1016/S1364-8152(98)00042-5, 373–384 p.

Chan, A.L.S. (2011). *Developing a modified typical meteorological year weather file for Hong Kong taking into account the urban heat island effect*. Building and Environment *46*, DOI : 10.1016/j.buildenv.2011.04.038, 2434–2441 p.

Elwy, I., Ibrahim, Y., Fahmy, M., and Mahdy, M. (2018). *Outdoor microclimatic validation for hybrid simulation workflow in hot arid climates against ENVI-met and field measurements*. Energy Procedia *153*, DOI : 10.1016/j.egypro.2018.10.009, 29–34 p.

EnergyPlus (2021). *https://energyplus.net/weather-search/wuhan*.

Hall, I.J., Prairie, R.R., Anderson, H.E., and Boes, E.C. (1978). *Generation of a typical meteorological year*, Sandia Labs., Albuquerque, NM (USA), SAND-78-1096C; CONF-780639-1, https://www.osti.gov/biblio/7013202.

Huang, K.-T., and Li, Y.-J. (2017). *Impact of street canyon typology on building's peak cooling energy demand: A parametric analysis using orthogonal experiment*. Energy and Buildings *154*, DOI : 10.1016/j.enbuild.2017.08.054, 448–464 p.

Huttner, S. (2012). *Further development and application ofthe 3D microclimate simulation ENVI-met*, PhD thesis, Johannes Gutenberg University Mainz.

Imhoff, M.L., Zhang, P., Wolfe, R.E., and Bounoua, L. (2010). *Remote sensing of the urban heat island effect across biomes in the continental USA*. Remote Sensing of Environment *114*, DOI : 10.1016/j.rse.2009.10.008, 504–513 p.

Lauzet, N., Rodler, A., Musy, M., Azam, M.-H., Guernouti, S., Mauree, D., and Colinart, T. (2019). *How building energy models take the local climate into account in an urban context – A review*. Renewable and Sustainable Energy Reviews *116*, DOI : 10.1016/j.rser.2019.109390, 109390 p.

Li, C., Zhou, J., Cao, Y., Zhong, J., Liu, Y., Kang, C., and Tan, Y. (2014). *Interaction between urban microclimate and electric air-conditioning energy consumption during high temperature season*. Applied Energy *117*, DOI : 10.1016/j.apenergy.2013.11.057, 149–156 p.

Li, H., Zhou, Y., Li, X., Meng, L., Wang, X., Wu, S., and Sodoudi, S. (2018). *A new method to quantify surface urban heat island intensity*. Science of The Total Environment *624*, DOI : 10.1016/j.scitotenv.2017.11.360, 262–272 p.

Li, X., Zhou, Y., Asrar, G.R., Imhoff, M., and Li, X. (2017). *The surface urban heat island response to urban expansion: A panel analysis for the conterminous United States*. Science of The Total Environment *605–606*, DOI : 10.1016/j.scitotenv.2017.06.229, 426–435 p.

Li, X., Zhou, Y., Yu, S., Jia, G., Li, H., and Li, W. (2019). *Urban heat island impacts on building energy consumption: A review of approaches and findings*. Energy *174*, DOI : 10.1016/j.energy.2019.02.183, 407–419 p.

López-Cabeza, V.P., Galán-Marín, C., Rivera-Gómez, C., and Roa-Fernández, J. (2018). *Courtyard microclimate ENVI-met outputs deviation from the experimental data*. Building and Environment *144*, DOI : 10.1016/j.buildenv.2018.08.013, 129–141 p.

Lowe, S.A. (2016). *An energy and mortality impact assessment of the urban heat island in the US*. Environmental Impact Assessment Review *56*, DOI : 10.1016/j.eiar.2015.10.004, 139–144 p.

Maheshwari, B., Pinto, U., Akbar, S., and Fahey, P. (2020). *Is urbanisation also the culprit of climate change? – Evidence from Australian cities*. Urban Climate *31*, DOI : 10.1016/j.uclim.2020.100581, 100581 p.

MOHURD (2010). *Design standard for energy efficiency of residential buildings in hot summer and cold winter zone*, Ed. China Architecture & Building Press.

Oke, T.R. (1982). *The energetic basis of the urban heat island (Symons Memorial Lecture, 20 May 1980).* Quarterly Journal, Royal Meteorological Society *108*, 1–24 p.

Pei, L. (2015). *The Study on Eco-design of High-rise Residential Buildings in Wuhan Based on Energy Simulation and Life Cycle Assessment*, Master thesis, Huazhong University of Science & Technology.

Peuportier, B. (1993). *COMFIE, logiciel pour l'architecture bioclimatique, quelques applications pour les vérandas*, In Journée technique GENEC (CEA), https://docplayer.fr/12225666-Comfie-logiciel-pour-la-conception-bioclimatique.html.

Peuportier, B. (2005). *Bancs d'essais de logiciels de simulation thermique*. In Journée Thématique IBPSA France - SFT 2005, Outil de Simulation Thermo-Aéraulique Du Bâtiment, (La Rochelle, France),.

Peuportier, B., and Blanc-Sommereux, I. (1990). *Simulation Tool with Its Expert Interface for the Thermal Design of Multizone Buildings*. International Journal of Solar Energy *8*, DOI : 10.1080/01425919008909714, 109–120 p.

Recht, T., Munaretto, F., Schalbart, P., and Peuportier, B. (2014). *Analyse de la fiabilité de COMFIE par comparaison à des mesures. Application à un bâtiment passif*. (Arras), 8 p.

Santamouris, M. (2015). *Analyzing the heat island magnitude and characteristics in one hundred Asian and Australian cities and regions*. Science of The Total Environment *512–513*, DOI : 10.1016/j.scitotenv.2015.01.060, 582–598 p.

Sharmin, T., and Steemers, K. (2017). *Understanding ENVI-met (V4) model behaviour in relation to environmental variables*. In PLEA 2017 Edinburgh: Design to Thrive, (Edinburgh: PLEA 2017), 2156–2164 p.

Skelhorn, C.P., Levermore, G., and Lindley, S.J. (2016). *Impacts on cooling energy consumption due to the UHI and vegetation changes in Manchester, UK*. Energy and Buildings *122*, DOI : 10.1016/j.enbuild.2016.01.035, 150–159 p.

Spitz, C. (2012). *Analyse de la fiabilité des outils de simulation et des incertitudes de métrologie appliquée à l'efficacité énergétique des bâtiments*, PhD thesis, Université de Grenoble.

Sun, Y., and Augenbroe, G. (2014). *Urban heat island effect on energy application studies of office buildings*. Energy and Buildings *77*, DOI : 10.1016/j.enbuild.2014.03.055, 171–179 p.

Thiers, S. (2008). *Bilans énergétiques et environnementaux de bâtiments à énergie positive*, PhD Thesis, École Nationale Supérieure des Mines de Paris.

Toparlar, Y., Blocken, B., Maiheu, B., and van Heijst, G.J.F. (2018). *Impact of urban microclimate on summertime building cooling demand: A parametric analysis for Antwerp, Belgium*. Applied Energy *228*, DOI : 10.1016/j.apenergy.2018.06.110, 852–872 p.

Tsinghua University (2020). *2020 Annual Report on China Building Energy Efficiency*, Ed. China Architecture & Building Press.

Tsoka, S., Tolika, K., Theodosiou, T., Tsikaloudaki, K., and Bikas, D. (2018). *A method to account for the urban microclimate on the creation of 'typical weather year' datasets for building energy simulation, using stochastically generated data*. Energy and Buildings *165*, DOI : 10.1016/j.enbuild.2018.01.016, 270–283 p.

Wei, Y., Huang, C., Li, J., and Xie, L. (2016). *An evaluation model for urban carrying capacity: A case study of China's mega-cities*. Habitat International *53*, DOI : 10.1016/j.habitatint.2015.10.025, 87–96 p.

Wu, N., Shi, P., Zhu, G., and Pan, X. (2017). *Changes of soil relative moisture content and influencing factor in the yangtze basin during 1992-2012*. Resources and Environment in the Yangtze Basin *26*, DOI : 10.11870/cjlyzyyhj201707006, 1001–1010 p.

Yang, X. (2012). *A simulation method for the effects of urban microclimate on building cooling energy use*, PhD Thesis, South China University of Technology.

Yang, A.X., Li, Y., Luo, Z., and Chan, P.W. (2016). *The urban cool island phenomenon in a high-rise high-density city and its mechanisms*. International Journal of Climatology *37*, DOI : 10.1002/joc.4747.

Yang, X., Zhao, L., Bruse, M., and Meng, Q. (2013). *Evaluation of a microclimate model for predicting the thermal behavior of different ground surfaces*. Building and Environment *60*, DOI : 10.1016/j.buildenv.2012.11.008, 93–104 p.

Yang, X., Yao, L., Jin, T., Peng, L.L.H., Jiang, Z., Hu, Z., and Ye, Y. (2018). *Assessing the thermal behavior of different local climate zones in the Nanjing metropolis, China*. Building and Environment *137*, DOI : 10.1016/j.buildenv.2018.04.009, 171–184 p.

Yang, X., Yao, L., Peng, L.L.H., Jiang, Z., Jin, T., and Zhao, L. (2019). *Evaluation of a diagnostic equation for the daily maximum urban heat island intensity and its application to building energy simulations*. Energy and Buildings *193*, DOI : 10.1016/j.enbuild.2019.04.001, 160–173 p.

Yang, X., Peng, L.L.H., Jiang, Z., Chen, Y., Yao, L., He, Y., and Xu, T. (2020). *Impact of urban heat island on energy demand in buildings: Local climate zones in Nanjing*. Applied Energy *260*, DOI : 10.1016/j.apenergy.2019.114279, 114279 p.

Zhou, W., Wang, J., and Cadenasso, M.L. (2017). *Effects of the spatial configuration of trees on urban heat mitigation: A comparative study*. Remote Sensing of Environment *195*, DOI : 10.1016/j.rse.2017.03.043, 1–12 p.

List of abbreviations

3D	Three-dimensional
DBES	Dynamic building energy simulation
E	East
HSJG	Haishan Jingu
MAE	Mean absolute error
N	North
RMSE	Root mean square error
S	South
TMM	Typical meteorological months
TMY	Typical meteorological year
UCI	Urban cool island
UCII	Urban cool island intensity
UHI	Urban heat island
UHII	Urban heat island intensity
W	West

List of symbols

I	Number of cells on x-axis in ENVI-met model
i	Hour number in a day
J	Number of cells on y-axis in ENVI-met model
j	Day number in a representative week
K	Number of cells on z-axis in ENVI-met model
n	Number of vertical cell
N_h	Number of different heights
P	Atmosphere pressure, Pa
P_0	Reference pressure , Pa
T	Temperature, °C or K
UCIdh	Urban cool island degree-hours, °C hours
UHIdh	Urban heat island degree-hours, °C hours

Superscripts and subscripts

abs	Absolute
air	Air
av	Average
ENVImet	ENVI-met results
EPW	EPW file
max	Maximal
pot	Potential temperature
re1	1st representative day
re2	2nd representative day

List of Greek letters

Δx	Resolution of cell on x-axis in ENVI-met model, m
Δy	The resolution of cell on y-axis in ENVI-met model, m
Δz	The resolution of cell on z-axis in ENVI-met model, m